Sequence Analysis and Fiber Properties of a Blend of Poly(ethylene terephthalate) and Poly(ethylene terephthalate-*co*-4,4′-bibenzoate)

Byung Min,[1,*] Satish Kumar,[1] Michael R. Hibbs,[2] Hongming Ma,[2] David M. Collard,[2] David A. Schiraldi[3]

[1]*School of Textile and Fiber Engineering, Georgia Institute of Technology, Atlanta, Georgia 30332-0295*
[2]*School of Chemistry and Biochemistry, Georgia Institute of Technology, Atlanta, Georgia 30332-0400*
[3]*Department of Macromolecular Science, Case Western Reserve University, Cleveland, Ohio 44106-7202*

Received 20 November 2003; accepted 3 March 2004
DOI 10.1002/app.20638
Published online in Wiley InterScience (www.interscience.wiley.com).

ABSTRACT: Blends of poly(ethylene terephthalate) (PET) and poly(ethylene terephthalate-*co*-4,4′- bibenzoate) (PETBB) are prepared by coextrusion. Analysis by ^{13}C-NMR spectroscopy shows that little transesterification occurs during the blending process. Additional heat treatment of the blend leads to more transesterification and a corresponding increase in the degree of randomness, *R*. Analysis by differential scanning calorimetry shows that the as-extruded blend is semicrystalline, unlike PETBB15, a random copolymer with the same composition as the non- random blend. Additional heat treatment of the blend leads to a decrease in the melting point, T_m, and an increase in glass transition temperature, T_g. The T_m and T_g of the blend reach minimum and maximum values, respectively, after 15 min at 270°C, at which point the blend has not been fully randomized. The blend has a lower crystallization rate than PET and PETBB55 (a copolymer containing 55 mol % bibenzoate). The PET/PETBB55 (70/30 w/w) blend shows a secondary endothermic peak at 15°C above an isothermal crystallization temperature. The secondary peak was confirmed to be the melting of small and/or imperfect crystals resulting from secondary crystallization. The blend exhibits the crystal structure of PET. Tensile properties of the fibers prepared from the blend are comparable to those of PET fiber, whereas PETBB55 fibers display higher performance. © 2004 Wiley Periodicals, Inc. J Appl Polym Sci 93: 1793–1803, 2004

Key words: blends; fibers; mechanical properties; NMR; polyesters

INTRODUCTION

The modification of poly(ethylene terephthalate) (PET) by copolymerization or blending with other polyesters, is an approach toward property enhancements that has been well studied.[1–6] Melt blending of two dissimilar polyesters is accompanied by transesterification and ultimately the formation of random copolyesters. Initial transesterification leads to formation of "blocky" copolymers, which then can further ester interchange to form random copolymers; this progression of structures has been demonstrated for blends of PET with poly(ethylene isophthalate),[5] poly(butylene terepthalate),[6,7] and poly(ethylene naphthalate) (PEN).[2,8] Liquid crystalline polymers (LCPs) have been blended with PET and other thermoplastics to obtain advanced materials that can be processed on conventional melt processing equipment.[9–11] Orientation of these LCP/thermoplastic blends often results in fibrous LCP morphologies that are described as self-reinforced composites. However, PET and LCPs are often incompatible and the rates of transesterification in melt blended samples of PET with liquid crystalline polyesters depend on the flexibility of the LCP.[12] The work described herein attempts to reinforce PET with a more compatible blend component.

^{13}C-NMR spectroscopy has been used to determine the relative amounts of differing monomer dyads in copolyesters[6,13] in cases in which ^{1}H-NMR spectroscopy is insensitive to copolymer sequence. An illustrative study showed that the substituted carbon atoms of the terephthalate and isophthalate units in poly(ethylene terephthalate-*co*-isophthalate) random copolymers give rise to a series of different peaks in the ^{13}C-NMR spectrum arising from dyad and triad sequences.[14] By comparing the integrated areas of those peaks, the authors were able to conclude that the relative amounts of dyad and triad sequences was in agreement with those predicted for a statistically random copolymer. These studies were restricted to the characterization of random copolymers, however, a potentially more interesting and challenging study involves analysis of nonrandom copolymer sequences, such as is discussed herein.

Correspondence to: D. A. Schiraldi (das44@po.cwru.edu).
*Permanent address: School of Advanced Materials and System Engineering, Kumoh National Institute of Technology, Kumi, Korea, 730-701.

The 4,4′-biphenyl moiety has been incorporated as a rigid structural unit as a diol and a diacid in both wholly aromatic and semiflexible polyesters. The development of an economical new synthesis of 4,4′-bibenzoic acid (BB) has led to new interest in copolymers prepared from this rigid monomer.[15] Poly(ethylene terephthalate-*co*-4,4′-bibenzoate) copolyesters (PETBB) have enhanced T_g, strength, modulus, and gas barrier properties compared to PET.[16,17] The modulus of fibers spun from random copolymers with 45–65 mol % bibenzoate approaches that of LCPs, which is ascribed to development of a frustrated liquid crystalline structure during the spinning process.[17] When samples of PET and the PETBB frustrated LCP were melt blended, the resultant blocky PET/PETBB copolymer was demonstrated to exhibit lower oxygen permeability than that of the isocompositional random PETBB material; these changes in transport properties were attributed to constraints imposed by connections between PET and PETBB blocks.[18] Given this behavior, in which the rigid-rod polyester influences the structure of PET, and the excellent properties of PETBB fibers, one could postulate that melt blending of PET and PETBB random copolymers might allow for the formation of blends and nonrandom copolymers with the superior properties of PETBB and the economy of PET, by analogy to the PET/LCP systems. In particular, an improvement in fiber modulus of PET without sacrificing tenacity would be attractive from an industrial view point, as would processing of the blend under normal melt spinning conditions.

In the present paper, we report the analysis of a coextruded blend of PET and PETBB. ^{13}C-NMR analysis is used to determine the amount of transesterification that occurs during extrusion, as well as the evolution of a random structure with further heat treatment. Differential scanning calorimetry is used to correlate thermal transitions of the blend with the degree of randomness. Having established the nature its structure, the fiber properties of a blend of PET and PETBB were then evaluated and related back to that structure.

EXPERIMENTAL

Materials and polymer blending

Pellets of PET and PETBB copolymers were supplied by KoSa and were produced from dimethyl terephthalate, dimethyl 4,4′-bibenzoate, and ethylene glycol by melt polymerization according to the published method.[18] The intrinsic viscosities (IV) of PET, PETBB15 (a copolymer containing 15 mol % BB), and PETBB55 (55 mol % BB) were 0.83, 0.90, and 0.55 dl/g, respectively, determined in 1% (w/w) dichloroacetic acid solutions at 25°C.

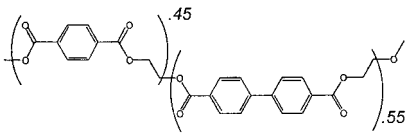

A 70/30 w/w blend of PET and PETBB55 was prepared using a Rheocord 90 twin-screw extruder (L/D = 9; 26 rpm rotor speed). The extruder temperature was 285°C and the residence time was 100 s. Following extrusion, samples of the blend were subjected to further heat treatment by placing them in a stirred glass vessel under nitrogen in a heated oil bath. The as- extruded blend had an IV of 0.69.

Melt spinning

Fiber spinning was carried out using a piston-driven small-scale fiber spinning system (Bradford Research Ltd.). Polymer samples were dried in vacuum at 80°C for 2 days before spinning. Fibers were spun at 270–310°C using a 250-μm-diameter spinneret. The extruded monofilament was solidified in room temperature air and then collected at various take-up speeds followed by drawing at 120°C and heat treatment at 150°C for 10 min.

Characterization

Copolymers were studied by ^{1}H-NMR spectroscopy to determine the ratio of terephthalate and bibenzoate units and by ^{13}C-NMR spectroscopy to determine the randomness of the sequence of the structural units. Samples were dissolved (ca. 50 mg/mL) in mixtures of TFA-*d* and $CDCl_3$ (approximately 5 : 95 v/v) and chemical shifts were measured with respect to internal tetramethylsilane (TMS). ^{1}H and ^{13}C spectra were acquired on a Bruker DMX 500 MHz instrument operating at 500.1 and 125.8 MHz, respectively. A spectral width of 31 kHz, relaxation delay of 2 s, and inverse gated decoupling were used to eliminate the nuclear Overhauser effect (nOe) and to optimize collection of spectra. A deconvolution program in the Bruker NMR software was used to integrate peaks in the ^{13}C spectra.

Differential scanning calorimetry (DSC) was performed using a TA Instruments Q100 differential scanning calorimeter to determine the glass transition, melting, and crystallization temperatures of the polymers and fibers at a scanning rate of $\pm$10°C/min. The isothermal crystallization tests for the blend were performed by quenching from the melt at 270°C. A cyclic heating rate of $\pm$3°C was applied for the modulated DSC scan.

The tensile properties of the fibers were determined using Rheometrics Scientific solids analyzer (RSA III). The gauge length and crosshead speeds for the tensile

tests were 25 and 10 mm/min, respectively. The monofilaments were mounted on paper tabs that facilitate fiber handling according to ASTM Method D3379. Prior to testing, the fiber diameters were determined by a laser diffraction method.[19]

Wide-angle X-ray diffraction was carried out on a multifilament bundle on a Rigaku 2D SAXS/WAXS Diffraction System (Rigaku Micromax-007, 45kV, 66 mA, $\lambda = 1.54$ Å).

RESULTS AND DISCUSSION

Molecular sequence and miscibility

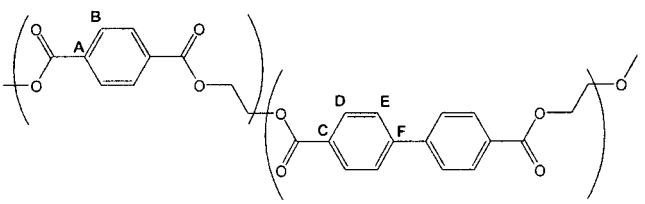

The ratio of terephthalate (T) units and bibenzoate (BB) units in each polymer sample was determined by ^{1}H-NMR spectroscopy and found to be in close agreement with the ratio of monomers charged in the polymerization mixture. The chemical shift of the carboxy-substituted aromatic carbons in the BB units (carbon C) are sensitive to the identity of adjacent diacid units. The BB–BB and BB–T dyads give rise to peaks at 128.77 and 128.70 ppm, respectively (Fig. 1). The relative amounts of these two dyads and the ratio of T to BB units can be used to determine the randomness, R,[18] of each sample. R has a theoretical value of 1.0 for a random copolymer, 2.0 for an alternating copolymer, and 0 for a physical blend of two homopolymers.[20] The value of R is 1.0 for random PETBB copolymers prepared by melt copolymerization of terephthalic acid, bibenzoic acid, and ethylene glycol. In contrast to mixing two homopolymers, each with $R=0$ to give a blend with $R = 0$, we blended a random copolymer (PETBB55) with $R = 1.0$ and a homopolymer (PET) with $R = 0$. Mixing these in a ratio of 70 : 30 (w/w) affords a blend with $R = 0.53$ (in the absence of transesterification). Upon heating to facilitate transesterification, the value of R for this blend should increase from 0.53 to 1.00 with the formation of a random copolymer containing 15 mol % BB (i.e., PETBB15).

Figure 2 shows that the value of R for the coextruded blend of PET and PETBB55 is 0.58 ± 0.03, indicating that a small amount of transesterification occurred during the extrusion process. Thus, the BB units are not randomly distributed throughout the sample and the blend resembles a block copolymer in which some of the blocks are rich in terephthalate units and some of the blocks are rich in bibenzoate units. Further randomization occurs when the coextruded blend is placed in a stirred reactor and heated above its melting point. As expected, R increases more rapidly at 300 than at 270°C, but the polymers are still not random after 3 h of mixing at these temperatures. The randomization processes at 300 and 270°C appear to follow first-order kinetics, with the former proceeding with a rate constant approximately three times that of the latter; given the limited data available, absolute rate constants and calculated activation energies would appear to be questionable here.

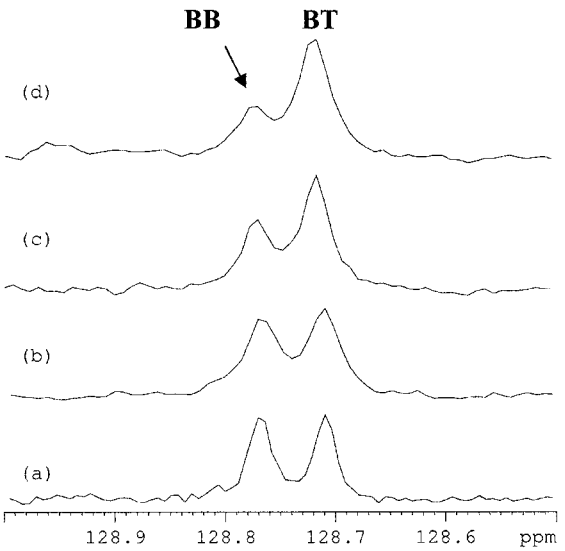

Figure 1 ^{13}C NMR spectra showing two peaks for the carbonyl-substituted carbon atom of the bibenzoate unit (carbon C in structure shown in text) arising from BB–BB and BB–T dyads in the blend: (a) as extruded, (b) after mixing at 270°C for 1 h, (c) after mixing at 270°C for 3 h, and (d) after mixing at 270°C for 6 h.

Whereas blending of dissimilar polymers, especially LCPs, often leads to formation of heterogeneous, cloudy blends, the as-extruded blend of PET and PETBB55 prepared in this study gave clear, homogeneous crystalline blends. Therefore, it is considered that these two components are miscible with each other even in the absence of transesterification. The possibility of micro- phase separation in PET/PETBB blends was recently suggested;[18] separation of PETBB blocks was proposed to be responsible for significant differences observed in cold-crystallization and cold-drawing behaviors compared to random PETBB copolymers containing equivalent levels of bibenzoate. The results of the present study are consistent with this proposal, though this phenomenon is not necessary to describe the observed fiber properties.

Thermal properties of the blend

DSC analysis was used to determine the influence of thermal treatment and sequence on the thermal tran-

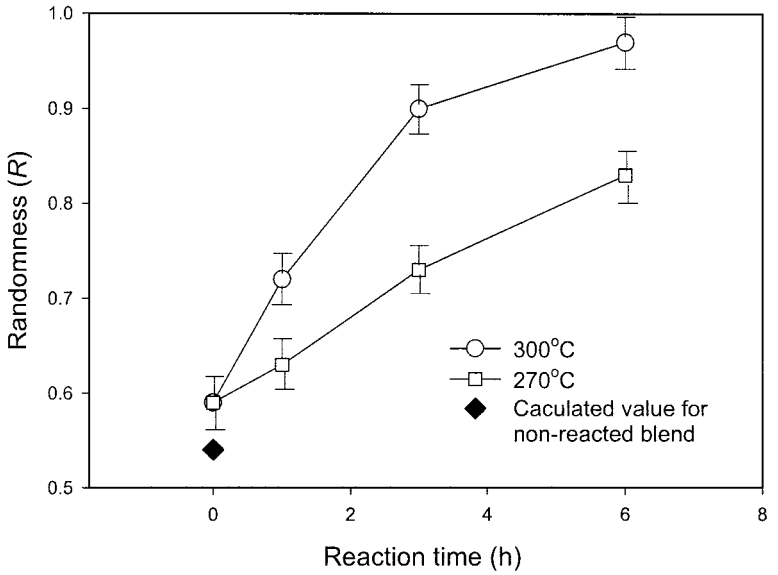

Figure 2 Change in the randomness, *R*, of the molten blend upon mixing. *R* for the sample after 0 h was measured three times with a standard deviation of 0.03 (indicated by the error bars). The same standard deviation is indicated on all the subsequent samples with the assumption that the errors are similar for all the samples.

sitions of the PET/PETBB55 (70/30) blend and are in good agreement with a previous report.[18] Figure 3 shows the heating cycles of polymers used in the blend and PETBB15, a random copolymer having similar composition to the blend. The random PETBB15 copolymer does not show crystallization during cooling and/or heating while the blend shows crystallization and melting during heating. The blend, however, does not show crystallization upon cooling from the melt. Though PETBB55 is reported to show faster crystallization than PET,[18] the blend crystallizes much more slowly than the two individual component polymers. PET and PETBB55 have similar melting points, 252 and 258°C, respectively. The as-extruded blend shows a strong melting endotherm at 240°C, whereas random PETBB15 is amorphous (Fig. 3). Thus, the PET segments in the blend are still long enough to crystallize after blending, and the two sequences PET and PETBB can cocrystallize (or the polymers phase separate on a length scale lower than the wavelength of light). The DSC curve of the as-extruded blend shows a glass transition temperature at 80°C, similar to that obtained for pure PET, while the T_g of PETBB55 (103°C) is not detectable.

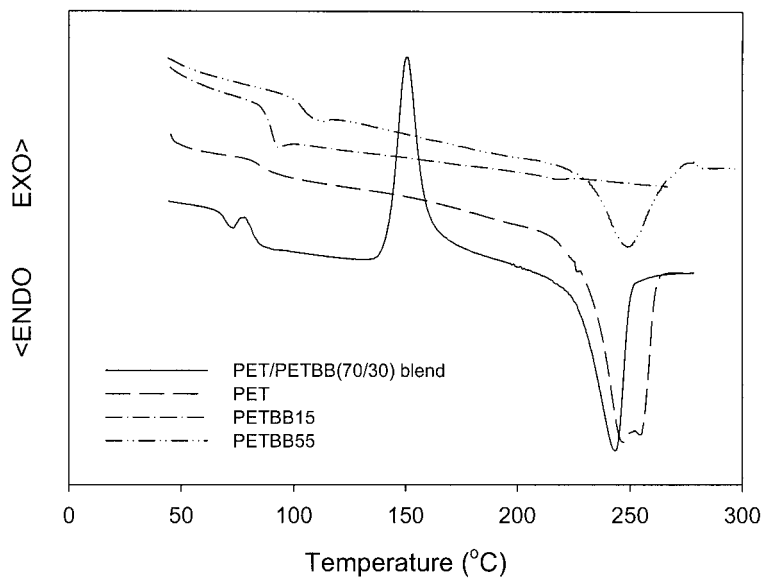

Figure 3 DSC thermograms (second heating) of PET, PETBB55, the PET/PETBB55 (70/30) blend, and PETBB15.

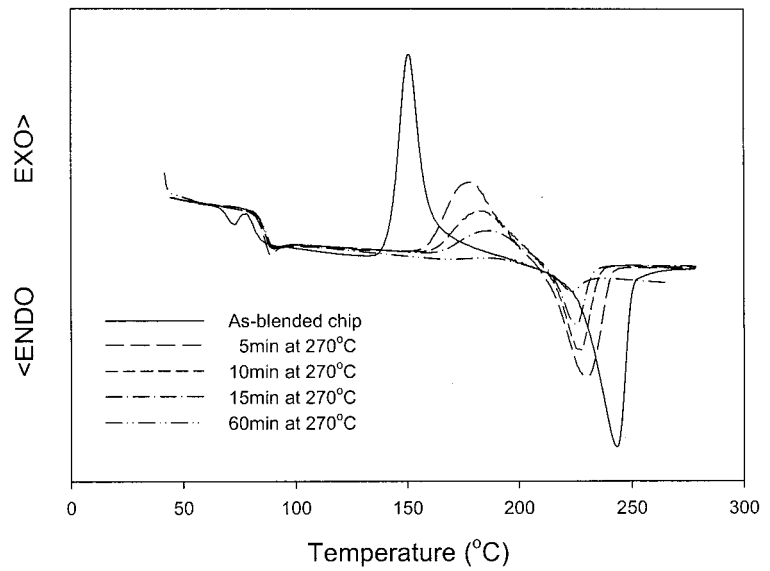

Figure 4 DSC thermograms of the PET/PETBB55 (70/30) blend after annealing at 270°C.

The thermal properties of the blend changed upon heat treatment. Figure 4 shows that the melting point (T_m) and the heat of fusion (ΔH_f) for the blend both decrease continuously upon heat treatment. A sample of the blend was cycled from 30 to 270°C in a DSC pan. As the BB units become more randomly distributed throughout the PET matrix, the PET segments become shorter, limiting crystallization. This is different from blends of PET with Rodrun™, in which the products of transesterification can cocrystallize with PET such that the heat of fusion does not change upon reactive blending.[12] With complete randomization, the PET/PETBB55 blend becomes random PETBB15, which does not crystallize. Blends of PET and PEN display similar behavior such that the degree of randomness is not a controlling factor to thermal properties of the blend after a certain level of transesterification has been achieved.[21,22]

Figures 5 and 6 plot the T_g, T_m, and ΔH_f of the blend as they change with heating time at 270°C. The thermal transitions change markedly over the first 15 min of heat treatment, during which the value of R only undergoes a small increase (Fig. 2). However, there is little change upon further heating and the blend does not crystallize after heating for more than 65 min. Comparing Figures 4, 5, and 6 with Figure 2, it is clear

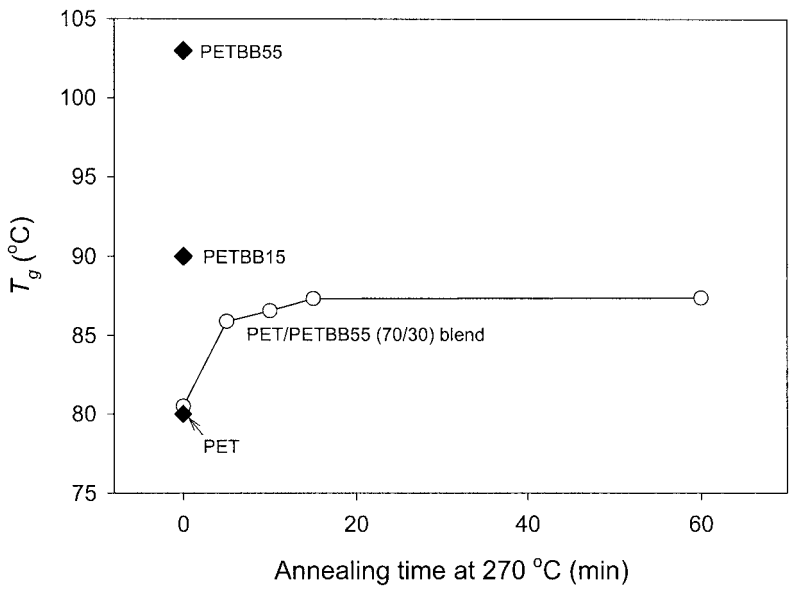

Figure 5 Changing of glass transition temperature of the PET/PETBB55 (70/30) blend with annealing time in melt.

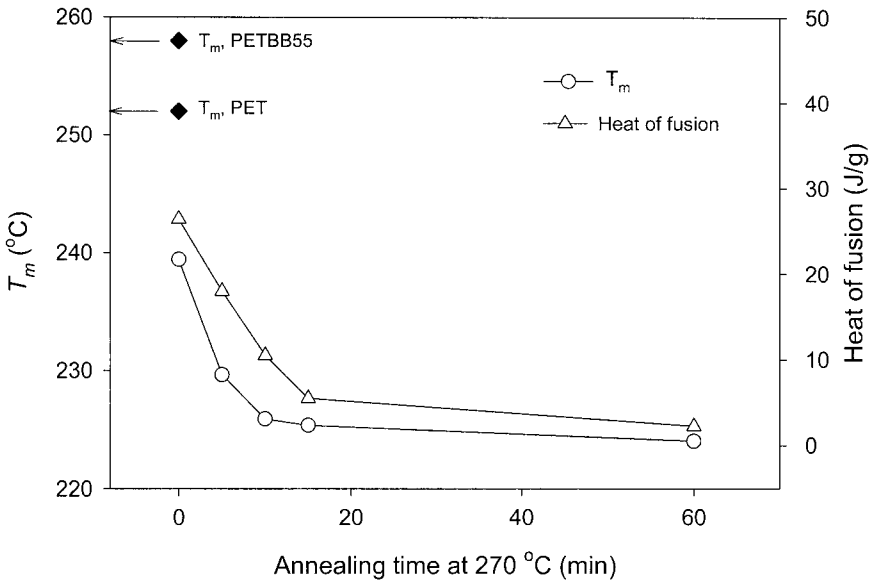

Figure 6 Changing of melting point and heat of fusion of the PET/PETBB55 (70/30) blend with annealing time in melt.

that randomization of the blend continues to occur long after the thermal transitions have reached constant values. This behavior can be accounted for assuming that a finite PET sequence length is required to form PET crystals. After a small amount of transesterification, the blend contains blocks of PET in which the average sequence length is too short to form crystals. The T_g of the blend increases with the time in the melt and levels off at 87°C, which is higher than that (83°C) calculated using the empirical Fox equation.[23,24]

Isothermal crystallization of the blend

The PET/PETBB blend does not show dynamic crystallization at cooling rate of 10–20°C from the melt, but isothermal crystallization from the melt was observed over a range of crystallization temperatures (T_c). Figure 7 plots the isothermal half-time for crystallization ($t_{1/2}$), defined as the time required to reach 50% of the maximum crystallinity. The $t_{1/2}$ shows a minimum at around 160°C. Isothermal crystallization from the melt for PET or random PETBB55 copolymer at the same range of T_c could not be obtained because melt crystallization of these polymers occurred too rapidly (i.e., during quenching). Thus, the blend has much lower crystallization rate than PET and PETBB55.

It is notable that three endothermic peaks were observed when the samples of the blend were heated

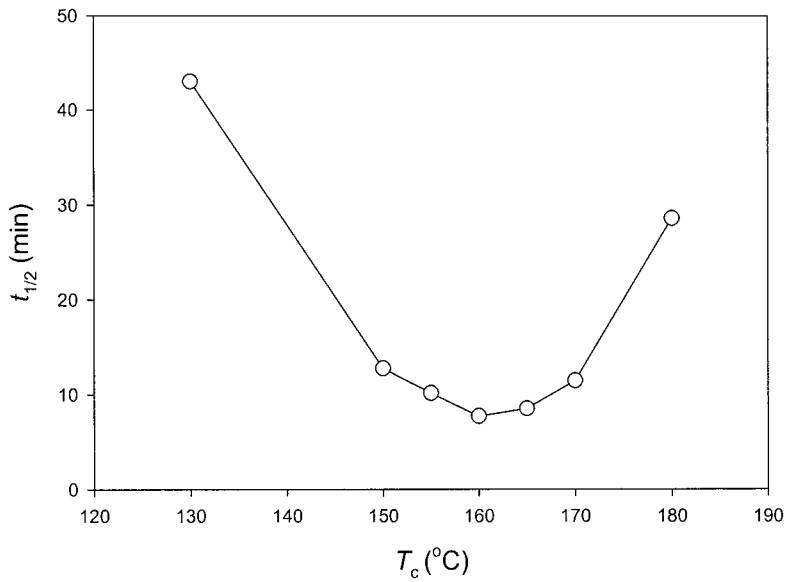

Figure 7 The half-time of crystallization, $t_{1/2}$, of the PET/PETBB55 (70/30) blend as a function of isothermal crystallization temperature.

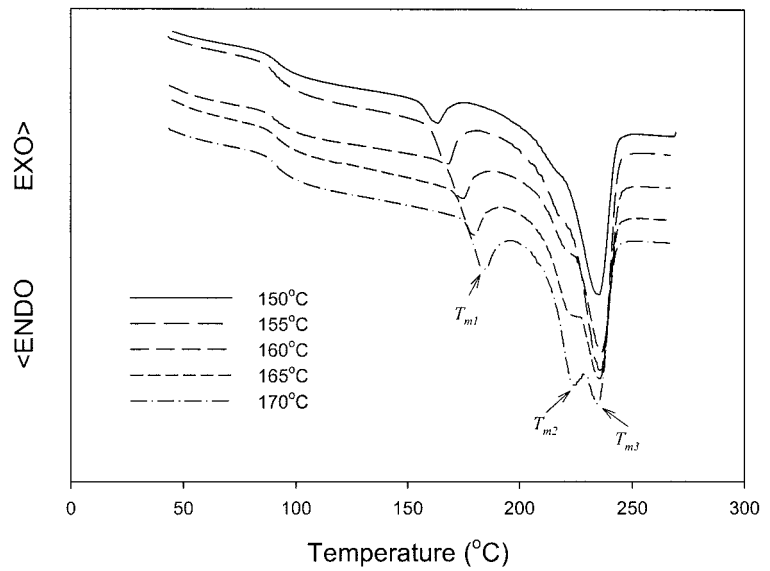

Figure 8 The multiple melting peaks in DSC scans at heating after crystallized isothermally at various crystallization temperatures.

after isothermal crystallization (Fig. 8). Each scan shows a small endothermic peak (T_{m1}) at about 15°C above T_c, followed by two melting peaks (T_{m2} and T_{m3}). A similar result was observed in a study of PET/PEN blend.[22] The peak positions are plotted in Figure 9 as a function of T_c. Lin and Koenig[25] suggested that the higher melting peak for PET/PEN blends, T_{m2}, results from the melting of the crystalline structure formed near the crystallization temperature. The T_{m2} shows a linear relationship with crystallization temperature to give an equilibrium melting point, T_m^o, of the as-blend of PET/PETBB55 (70/30) at 272°C. T_{m3} remains constant at *ca.* 236°C irrespective of T_c.

The small endothermic peak, T_{m1}, can result from physical aging or melting of small and/or imperfect crystals. The amorphous structure in a polymer spontaneously changes toward an equilibrium structure when kept at a fixed temperature.[26] For the purpose of a more detailed understanding of T_{m1}, a modulated DSC (MDSC) was used to analyze the isothermally crystallized samples. Deconvolution of the resultant heat flow profile during the cyclic heating provides not only the "total" heat flow obtained from conventional DSC but also separates that "total" heat flow into its heat capacity-related (reversible) and kinetic (nonreversible) components.[27] Heat flow correspond-

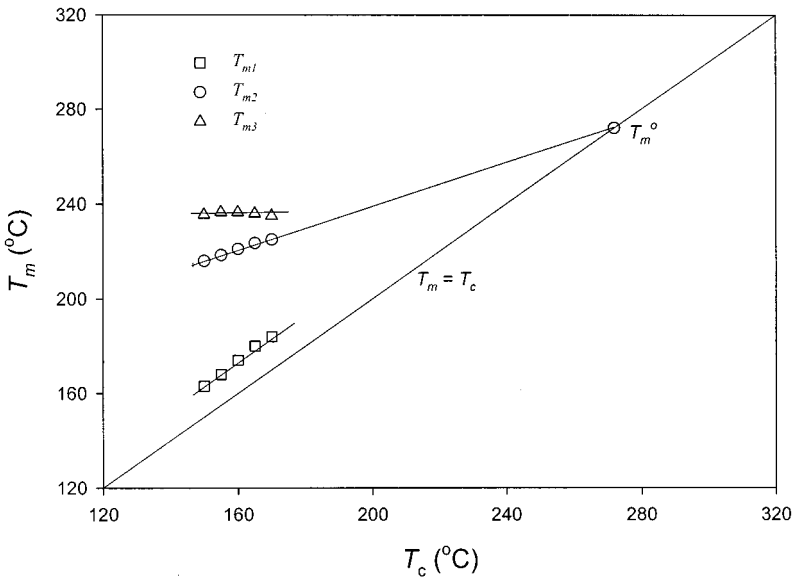

Figure 9 Plots of three melting peak temperatures as a function of isothermal crystallization temperature.

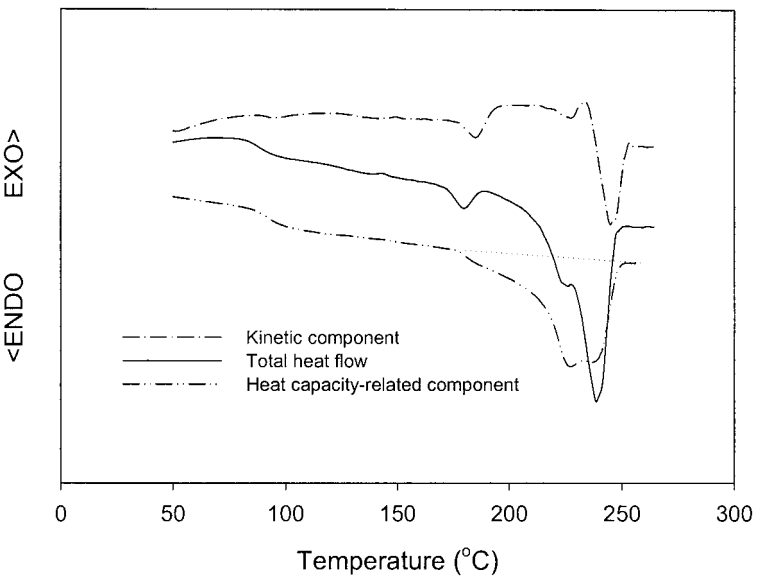

Figure 10 Typical modulated DSC curves for the sample crystallized isothermally at 170°C.

ing to crystallization is nonreversible while that of melting is reversible. The reversible component of the MDSC scan represented in Figure 10 shows that the crystal melting begins at T_{m1} and occurs continuously. This implies that this peak relates to melting of small crystals. Another DSC heating scan was performed for the sample aged isothermally at two different temperatures in succession. Program I held the sample for 7 min at 170°C from the melt, which is shorter than $t_{1/2}$ at this temperature, followed by 40 min at 140°C. Program II held the sample for 30 min at 170°C (enough time for secondary crystallization in this sample) and 40 min at 140°C, as represented in Figure 11. Thus, there was much less chance for the secondary crystallization at 170°C by Program I than by Program II, while the samples experienced the same amount of aging at 140°C in both programs. Figure 11 shows the DSC heating curves obtained after treatment of the samples by these two thermal programs. The peak areas are not proportional to the isothermal time at each temperature. The peaks at 140°C show different areas despite the same aging times, which implies that this peak does not result from physical aging. Furthermore, the shift of the peak at 170°C in Program II indicates that this peak is closely related to the secondary crystallization. Results of MDSC and isothermal treatment at two successive T_c sclearly shows that T_{m1} results from small and/or imperfect crystals resulting from a secondary crystallization process during isothermal crystallization, as Lin and Koenig[25] suggested for PET/PEN.

Orientation-induced crystallization in the fibers

The effect of temperature on the spinning behavior of PET/PETBB55 (70/30) blend was investigated. The blend showed good spinnability from as low as 270°C up to 310°C. The as- spun fiber (without further treatment after spinning) showed the same T_m as that of the as-extruded blend chip, suggesting that little transesterification occurred during fiber spinning. In general, fiber crystallinity tends to increase with increasing orientation (as a result of orientation-induced crystallization). Figure 12 shows the effect of spinning temperature on the crystallization of PET/PETBB55 (70/30) blend. Figure 13 shows the effect of spin draw ratio (*SDR*), defined according to eq. (2), on the crystallization of the blend fiber spun at 270°C. Both the heat of fusion and the on-line crystallinity, defined according to eq. (1), decrease with increasing spinning temperature. The cold crystallization peak position of the fibers gradually decreases with increase of *SDR* up to *SDR* = 550 and then levels off. These somewhat surprising results may suggest that under conditions of high orientation stress (low viscosity resulting from high melt temperatures or from high draw ratios), the PET/PETBB blends form highly oriented, but not necessarily highly crystalline structures. The high levels of birefringence reported previously during PETBB fiber spinning is consistent with such strain-induced orientation of rigid-rod polyesters.[17]

$$\text{On-line crystallinity (\%)} = (\Delta H_f - \Delta H_{cc})/\Delta H_f \times 100 \quad (1)$$

ΔH_f and ΔH_{cc} denote the heats of fusion and cold crystallization of the fibers, respectively.

$$SDR = V_{TU}/V_o \quad (2)$$

V_o and V_{TU} denote the velocity at the exit of the spinneret hole and take-up velocity, respectively.

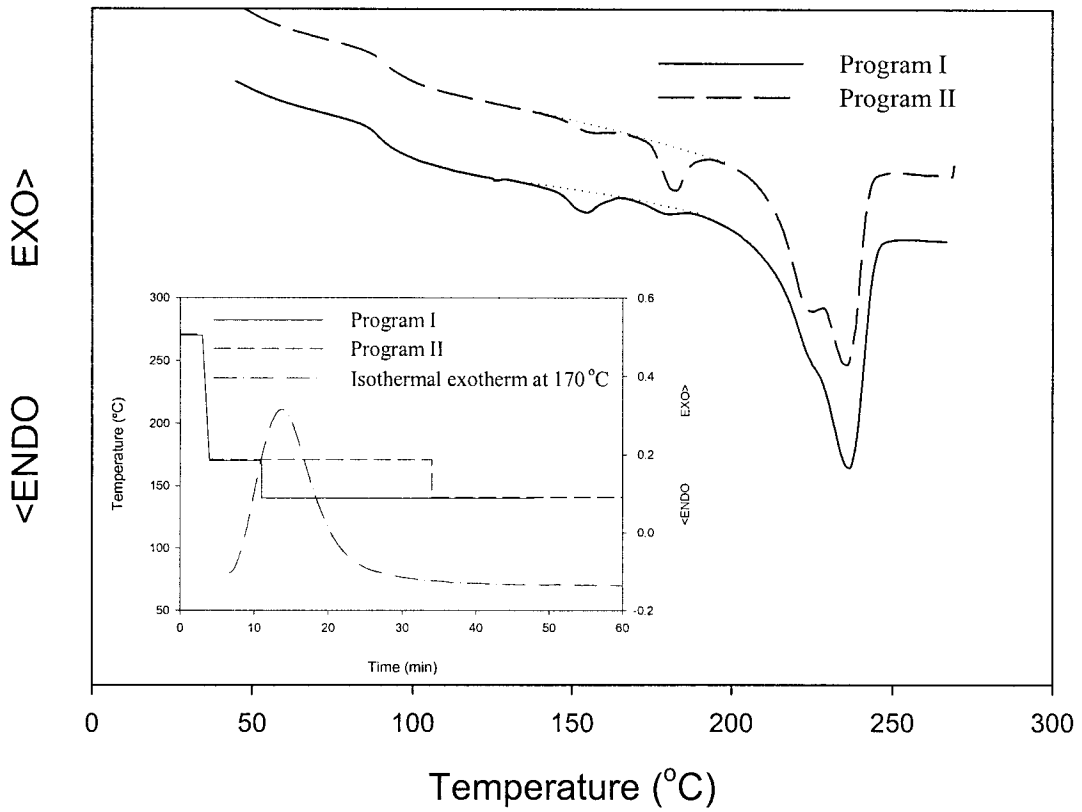

Figure 11 DSC heating scans after isothermal crystallization at two different temperatures in succession. Program I: 3 min at 270°C, 7 min at 170°C, and 30 min at 140°C; Program II: 3 min at 270°C, 30 min at 170°C, and 30 min at 140°C.

Crystal structure and mechanical properties of the fibers

Figure 14 represents WAXD patterns for the fibers that were drawn and heat-treated fibers. Fibers of both the PET/PETBB55 (70/30) blend and PETBB15 random copolymer exhibit the well-known, triclinic crystal structure of PET fiber itself. In contrast, fibers of PETBB55 random copolymer show the same crystal structure as that of poly(ethylene 4,4′-bibenzoate) (PEBB).[17,28,29] Fibers of the blend do not show the

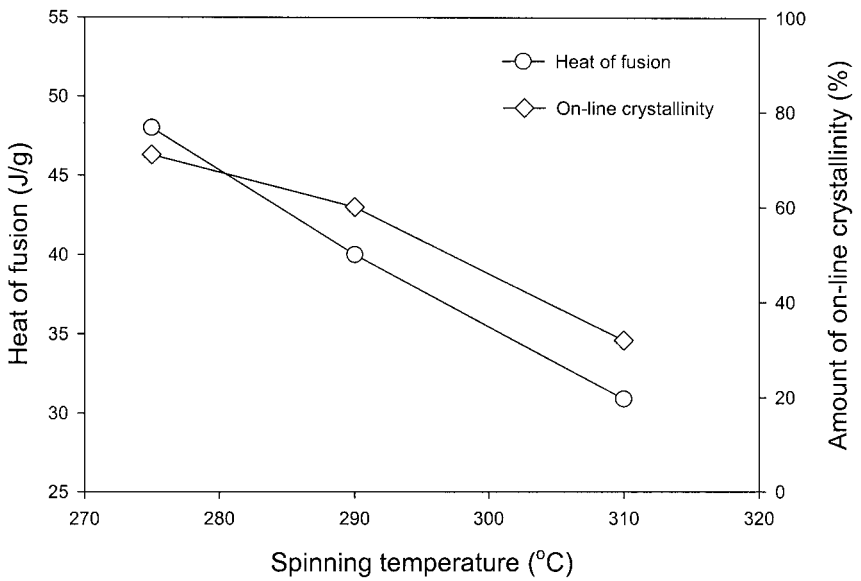

Figure 12 Effect of spinning temperature on the crystallization of the PET/PETBB55 (70/30) blend.

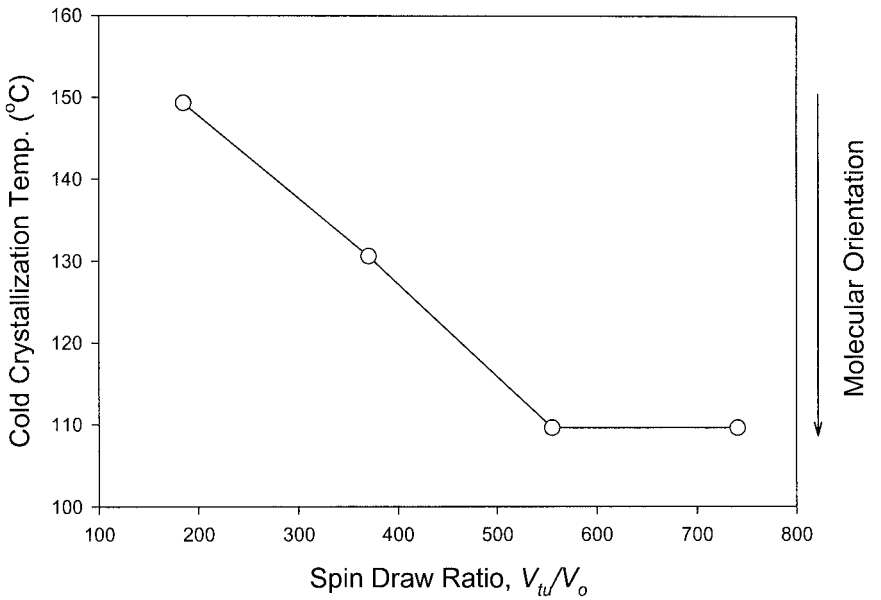

Figure 13 Effect of spin draw ratio on the cold crystallization of the PET/PETBB55 (70/30) blend fiber spun at 270°C.

crystalline structure of PETBB55, though it still has a blocky structure. In recently published film studies of PET/PETBB blends, two possibilities were raised to explain the observed blend crystallization phenomena: (1) that PETBB55 domains within the blend are too small for crystal nucleation or (2) that PETBB blocks are accommodated within the PET unit cell.[18] The data contained in this fiber study certainly are consistent with the first explanation, that the blend does not have a long enough block length for the formation of PEBB crystals, and therefore the PET units present within the PETBB blend domains crystallize with the PET component of the blend. While the alternative explanation of PETBB domains being accommodated within the PET unit cell cannot be excluded by the present work, no further support of this more complex explanation is provided.

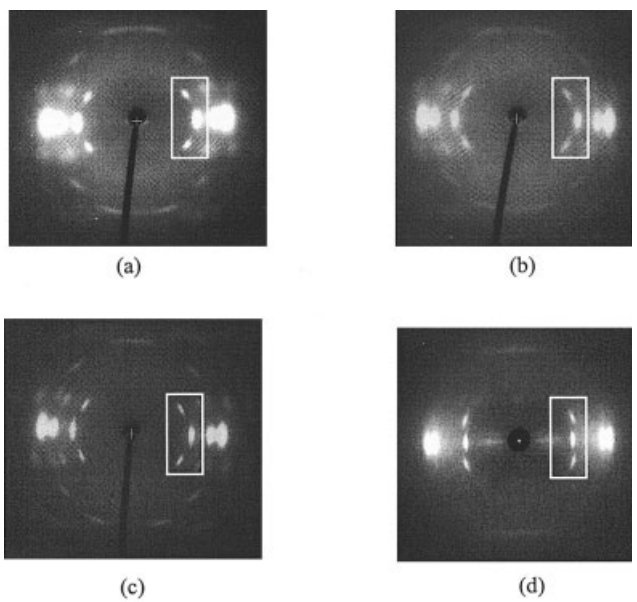

Figure 14 Wide-angle X-ray diffraction patterns of (a) PET, (b) PETBB15, (c) the PET/PETBB55 (70/30) blend, and (d) PETBB55. The diffraction arcs in the white rectangles show that the blend does not have a PETBB55 crystal structure but has a PET structure.

The tensile properties of the fibers of the blend and copolymers are compared in Figure 15. It has already been reported that drawn and heat-treated fibers of PETBB15 random copolymer show tensile properties comparable to those of PET homopolymer fibers, while the PETBB55 random copolymer fiber exhibits modulus values as high as 41 GPa.[17] It was also reported that, while no evidence of liquid crystallinity in the PETBB55 copolymer was observed from thermal, optical, and rheological methods, the copolymers display interesting processing characteristics and can be considered to be frustrated liquid crystals.[17] The present work shows that the PET/PETBB block structure offers no improvement in tensile strength or modulus over PET homopolymer or a random copolymer containing the same bibenzoate concentration. Consideration of the tensile properties of the fibers with their WAXD patterns suggests that the formation of the PEBB crystal structure in the fiber is required to show high performance for this blend but that the ethylene bibenzoate block in the blend is too short to crystallize. So, unlike the oxygen permeation results for PET/PETBB blends, which were previously shown to be sensitive to copolymer blockiness,[18] the fiber mechanical properties of PET/PETBB blends appear to be insensitive to monomer sequence at this level of substitution.

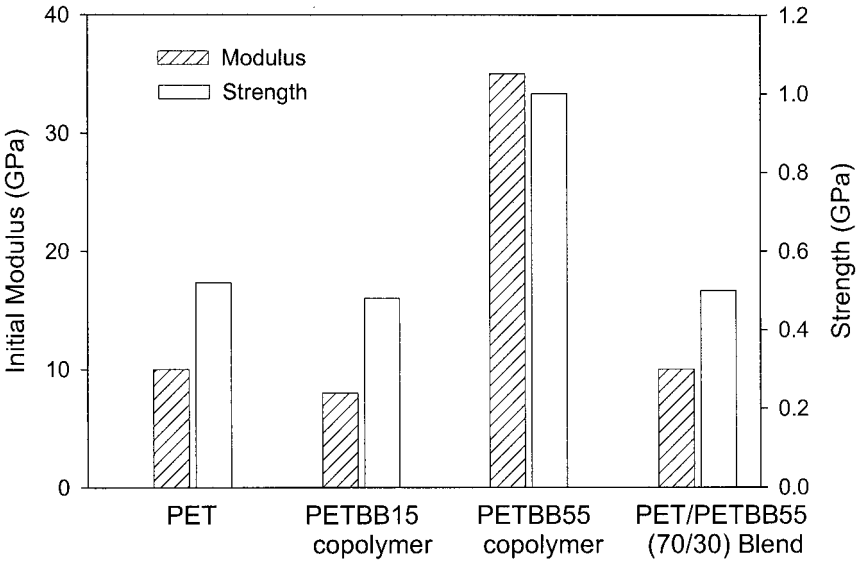

Figure 15 Comparison of the tensile properties of the blend with PET and copolymers.

CONCLUSION

PET and PETBB55 are miscible and can be melt blended to give nonrandom semicrystalline blends. Thermal properties of the blend approach those of a random copolymer after very little transesterification takes place. Sequence analysis by ^{13}C-NMR spectroscopy allows us to confirm that transesterification occurs during melt blending and also shows that the T_g and T_m values only change significantly during the early part of the blending process. Results of MDSC of copolymers crystallized at two temperatures indicate that small and/or imperfect crystals result from a secondary crystallization process during isothermal crystallization. The PET/PETBB55 (70/30) blend exhibited the crystal structure of PET. Tensile properties of the blend fiber are comparable to those of PET fiber, suggesting that the ethylene bibenzoate blocks in the blend are too short to form PEBB crystals of a size necessary to obtain high fiber mechanical performance.

ACKNOWLEDGMENT

We thank KoSa for support of our research programs in functional and structural polyesters, and Professors Anne Hiltner and Eric Baer, of Case Western Reserve University, for many useful conversations while collaborating in this area of polyester structure–property relationships.

References

1. Shepherd, F. A.; Ronald, R. L. (to Eastman Kodak Co.) U.S. Patent 5 006 613 (1991).
2. Stewart, M. E.; Cox, A. J.; Taylor, D. M. Polymer 1993, 34, 4060.
3. Aoki, Y.; Li, L.; Amari, T.; Nishimura, K.; Arashiro, Y., Macromolecules 1999, 32, 1923.
4. Patcheak, T. D.; Jabarin, S. A., Polymer 2001, 42, 8975.
5. Ha, W. S.; Chun, Y. K.; Jang, S. S.; Rhee, D. M.; Park, C. R., J Polym Sci, Part B: Polym Phys 1997, 35, 309.
6. Kim, J. H.; Lyoo, W. S.; Ha, W. S. J Appl Polym Sci 2001, 82, 159.
7. Matsuda, H.; Asakura, T.; Miki, T. Macromolecules 2002, 35, 4664.
8. Ihm, D. W.; Park, S. Y.; Chang, C. G.; Kim, Y. S.; Lee, H. K. J Polym Sci, Part A: Polym Chem 1996, 34, 2841.
9. Brown, C. S.; Alder, P. T. In Polymer Blends and Alloys; Folkes, M. J.; Hope, P. S., Eds.; Blackie Academic: Glasgow, 1993; Chap. 8, pp 193–227.
10. Baird, D. G.; McLeod, M. A. In Polymer Blends Volume 2: Performance; Paul, D. R.; Bucknall, C. B., Eds.; Wiley: New York, 2000; Chap. 32, pp 429–453.
11. Chang, J.; Jo, B.; Jin, J. J Polym Eng Sci 1995, 35, 1605.
12. Magagnini, P.; Tonti, M. S.; Masseti, M.; Paci, M.; Minkova, L. I.; Miteva, T. Polym Eng Sci 1998, 38, 1572.
13. Muhlebach, A.; Johnson, R. D.; Lyerla, J.; Economy, J. Macromolecules 1988, 21, 3115.
14. Martinez de Ilarduya, A.; Kint, D. P. R.; Munoz-Guerra, S. Macromolecules 2000, 33, 4596.
15. Sherman, S. C.; Iretskii, A. V.; White, M. G.; Schiraldi, D. A. Chem Innov. 2000, 30, 25.
16. Hu, Y. S.; Rogunova, M.; Schiraldi, D. A.; Hiltner, A.; Baer, E. J Appl Polym Sci 2002, 86, 98.
17. Ma, H.; Hibbs, M. R.; Collard, D. M.; Kumar, S.; Schiraldi, D. A. Macromolecules 2002, 35, 5123.
18. Liu, R. Y. F.; Hu, Y. S.; Hibbs, M. R.; Collard, D. M.; Schiraldi, D. A.; Hiltner, A.; Baer, E J Polym Sci Polym Phys Ed 2003, 41, 289.
19. Perry, A. J.; Lenichen, B.; Eliasson, B. J Mater Sci 1974, 9, 1376.
20. Ibbett, R. N. NMR Spectroscopy of Polymers; Blackie Academic and Professional: London, 1993; p 50.
21. Shi, Y.; Jabarin, S. A. J Appl Polym Sci 2001, 80, 2422.
22. Shi, Y.; Jabarin, S. A. J Appl Polym Sci 2001, 81, 11.
23. Fox, T. G.; Loshaek, S. J Polym Sci 1955, 15, 371.
24. Fox, T. G. Bull Am Phys Soc 1956, 1, 123.
25. Lin, S. B.; Koenig, J. L. J Polym Sci Polym Symp 1984, 71, 121.
26. Kovacs, A. J. Fortschr Hochpolym-Forsch 1963, 3, 394.
27. Q100 DSC Manual, supplied by TA Instruments, 2001.
28. Wendling, J.; Gusev, A. A.; Suter, U. W.; Braam, A.; Leemans, L.; Meier, R. J.; Aerts, J.; Heuvel, J. V. d.; Hottenhuis, M. Macromolecules 1999, 32, 7866.
29. Li, X.; Brisse, F. Macromolecules 1994, 27, 2276.